Abstract

Shipton, Matthew K. The Use of Biodegradable Poly(β-amino ester) and Poly(β-amino amide) Microspheres as an Experimental Therapeutic Delivery Vector for Selective Cancer Cell Targeting. (Advised by Daniel L. Feldheim)

The design, synthesis, and use of new biodegradable polymers for drug delivery applications is an area of ever increasing interest. Polymeric drug delivery systems have several advantages compared to conventional drug delivery methods such as liposomes and antibodies. Since liposomes are spherical vessels made of phosphorolipids, they are tiny particles which can be taken up by the macrophages. Antibodies, meanwhile, have the disadvantage that most receptor sites on tumor cells are also present on healthy cells. Several of these advantages include localized delivery, improved drug efficiency, and drug protection of certain medications which may degrade rapidly when inside the body.

Poly(β-amino esters) and Poly(β-amino amides) are ideal polymers for the encapsulation, delivery, and release of various therapeutic agents to cancer cells, which have an acidic extra cellular pH level, near 6.8[1]. Poly(β-amino esters) and Poly(β-amino amides) are specifically designed to degrade by hydrolysis of the ester and amide bonds respectively, in the polymer backbone. Microspheres of Poly(β-amino ester) and Poly(β-amino amide) are formed via a double emulsion process using Rhodamine B-Isothiocyanate (RBITC) labeled Bovine Serum Albumin (BSA) as the encapsulate. The fluorescence intensity of the RBITC-BSA released from the polymer sphere was measured as a way of testing polymer backbone hydrolysis. The polymer microspheres were placed into different solutions of

varying pH ranges. The pH range extended from pH 5.5 to pH 7.4. The hydrolyzed polymer byproducts were removed and the resulting supernatant tested for fluorescence intensity. The results showed polymer hydrolysis and release of labeled BSA at pH 6.8 and lower. .

The Use of Biodegradable Poly(β-amino ester) and Poly(β-amino amide) Microspheres as an Experimental Therapeutic Delivery Vector for Selective Cancer Cell Targeting.

By

Matthew K. Shipton

A Thesis Submitted to the Graduate Facility of
North Carolina State University
in Partial Fulfillment of the
Requirements for the Degree of
Masters of Science

Department of Chemistry

Raleigh, North Carolina
August 12, 2004

Approved by:

_____
Dr. Daniel L. Feldheim, Chair of Advisory Committee

_____ _____
Dr. Edmond F. Bowden Dr. David A. Shultz

I dedicate this Thesis to my loving friends and family,

It has been a long bumpy road with many ups and downs,

But through it all, you were always there.

Biography

Matthew K. Shipton was born February 17, 1979 in Sharon Pennsylvania. He is the son of Larry and Dr. Sharon Shipton. Matthew spent all of his childhood in the small Western Pennsylvania town of Grove City. Matthew received his primary education from Highland Park Elementary School and Grove City Middle School. He attended Grove City Area Senior High School, earning both academic and athletic scholarships before graduating in 1997. In the fall of 1997 Matthew enrolled at Youngstown State University earning the Division I-AA National Championship in football with his team in 1997. He was also a member of the 1999 Division I-AA National Finalist team. Matthew graduated from Youngstown State in 2001 earning a Bachelor of Science in Chemistry and minor degrees in the area of Philosophy, Mathematics, and Economics. Through his hard work and dedication Matthew earned a Teaching Assistantship to attend North Carolina State University. He moved to Raleigh in August of 2001. In December of 2001 Matthew began his graduate research working under the advisement of Daniel L. Feldheim. Through his hard laboratory work and his problem solving ability he was promoted to Research Assistant after his first year under Dr. Feldheim.

Matthew received his Master of Science in Chemistry degree in December of 2004.

Acknowledgements

First I would like to acknowledge my parents for their love and support. Without which I would not be where I am today. I would like to thank them for everything they have done for me both financially and emotionally. Thank you Mom and Dad!

Second, I would like to Acknowledge my adviser Dr. Daniel L. Feldheim for all of his help and encouragement. Dan invited me into the group with open arms and has been there throughout. He has made this experience not only an educational one but an enjoyable one as well. Dan, best of luck with your company, who knows maybe some day I will work for you again or vice versa.

Next, I would like to acknowledge my friends here at State. JD and DG, for all of the memorable moments outside of the department my first two years, Justyna, for the wild parties and always being there when I needed someone to talk to, and Dana for always having an open ear. I would also like to give a special acknowledgement to Joe Ryan. Joe is a great friend who was always there whenever I needed anything. I am sure there are some of you whom I forgot to acknowledge but from the bottom of my heart, thank you.

Finally, I would like to acknowledge my crew of friends back in Y-town. The Chrystal's Marty, Pat, Little Jeffery, Nora, and Jeff; to all of you I am very grateful. You all helped me though a very dark period of my life and I will never be able to repay you for what you did, I am eternally grateful.

I would like to give a special acknowledgement to the Dewberry's for being my family away home, Bonnie and Richard for all of the good meals and times at the lake, Stephanie, Timmy, and Joel for treating me like I was their own brother. I would also

like to acknowledge Timmy King for teaching me how to cook and always being there.

My final acknowledgement is to Ryan Dewberry. Dewbs you truly are the greatest friend a person could have, you have done more for me then I could ever possibly payback, thank you for everything.

Table of Contents

List of Figures……VII

List of Tables……X

1. Introduction……..1

2. Synthesis of Poly(β-amino esters) and Poly(β-amino amides)……6

3. Therapeutic Encapsulation…….8

4. Polymer degradation and Release Studies……11

5. Conclusion…….....18

6. References……19

7. Appendices……20

List of Figures

Chapter 1

Figure 1 Schematic of polyamine hydrolysis vs. polyester hydrolysis…….3

Chapter 2

Figure 2 General scheme of a Michael addition…….6

Chapter 3

Figure 3 SEM of RB-BSA loaded microspheres cluster……...10

Figure 4 SEM of signal RB-BSA loaded microspheres cluster…10

Chapter 4

Figure 5 Fluorescence release profile of poly(1,4 BDDA-co-2-AE) polymer microsphere containing rhodamine β-conjugated BSA..13

Figure 6 Fluorescence release profile of poly(1,4 BDDA-co-TMDP) polymer microsphere containing rhodamine β-conjugated BSA……14

Figure 7 Fluorescence release profile of poly(1,4 MBAA-co-TMDP) polymer microsphere containing rhodamine β-conjugated BSA……15

Appendices

Figure 8 Structure of Poly(1,3-butanediol diacrylate-co-2-aminoethanol)……20

Figure 9 ^{1}H NMR of Poly(1,3-butanediol diacrylate-co-2-aminoethanol)……20

Figure 10 ^{13}C NMR of Poly(1,3-butanediol diacrylate-co-2-aminoethanol)……20

Figure 11 Structure of Poly(1,4-butanediol diacrylate-co-2-aminoethanol)……21

Figure 12), ^{1}H NMR of Poly(1,4-butanediol diacrylate-co-2-aminoethanol)……21

Figure 13 and ^{13}C NMR of Poly(1,4-butanediol diacrylate-co-2-aminoethanol)……21

Figure 14 Structure of Poly(N,N-methylene bisacrlyamide-co-2-aminoethanol)……22

Figure 15 ^{1}H NMR of Poly(N,N-methylene bisacrlyamide-co-2-aminoethanol)……22

Figure 16 ^{13}C NMR of Poly(N,N-methylene bisacrlyamide-co-2-aminoethanol)……22

Figure 17 Structure of Poly(1,3-butanediol diacrylate-co-trimethylene dipiperidine)……..23

Figure 18 ^{1}H NMR of Poly(1,3-butanediol diacrylate-co-trimethylene dipiperidine)……..23

Figure 19 Structure of Poly(1,4-butanediol diacrylate-co-trimethylene dipiperidine)……..24

Figure 20 ^{1}H NMR of Poly(1,4-butanediol diacrylate-co-trimethylene dipiperidine)……..24

Figure 21 ^{13}C NMR of Poly(1,4-butanediol diacrylate-co-trimethylene dipiperidine)……..24

Figure 22 Structure of Poly(N,N-methylene bisacryamide-co-trimethylene dipiperidine)……..25

Figure 23 ^{1}H NMR of Poly(N,N-methylene bisacryamide-co-trimethylene dipiperidine)……..25

Figure 24 Structure of Poly(1,3-butanediol diacrylate-co-benzyl amine)……26

Figure 25 ^{1}H NMR of Poly(1,3-butanediol diacrylate-co-benzyl amine)……26

Figure 26 ^{13}C NMR of Poly(1,4-butanediol diacrylate-co-benzyl amine)……26

Figure 27 Structure of Poly(1,4-butanediol diacrylate-co-benzyl amine)……27

Figure 28 ^{1}H NMR of Poly(1,4-butanediol diacrylate-co-benzyl amine……27

Figure 29 ^{13}C NMR of Poly(1,4-butanediol diacrylate-co-benzyl amine)...……27

List of Tables

Table 1 Release percentages of RB-BSA from polymer microspheres……12

Table 2 Six day release profile of poly(MBAA-co-TMDP)…....16

Table 3 Release profile of poly(1,4-BDDA-co-TMDP)……..16

Chapter 1

Evidence accumulated over the last 50 years has shown human tumor pH to be, on average, lower then pH of healthy tissue.[1] Breast cancer cells especially are characterized by their highly invasive nature which enables them to metastasize to distant sites.[2] Metastasis in solid tumors is associated with increased expression of extracellular proteases and tissue remodeling. Lysosomal proteases, cathepsin D for example, are over expressed by cancer cells, which secrete them in an inactive pro-enzyme form,[3] these pro-enzymes need to be activated and freed from endrogeneous inhibitors to become functional. Increased secretion of pro-enzymes occurs most often in transformed cells. In breast cancer, increased synthesis and secretion of pro-cathepsin D is stimulated by estrogen[2]. Increased cathepsin D concentration is associated with greater risk of developing metastases in breast cancer patients. Although the activation of cathepsin does occur intracellularly in the acidic phagosomes and lysosomes, it may, in suitable conditions occur extracellularly, allowing the cathepsin a role in the degradation of the extracellular matrix.

There are two different causes behind the decreased pH of the extracellular matrix in cancer cells. The first is the increased lactic acid production and the second is the increase in carbon dioxide inside the cell. The poor vasculature in tumor tissues results in a non-homogenous blood flow, thus causing a non-uniform nutrient delivery. This poor nutrient delivery causes the cells to generate energy from an increase in the rate on anaerobic gylcolysis. The increased rate of anaerobic glycolysis causes an increase in lactic acid production in poorly perfused regions.[4] Since, the blood flow has now been reduced, the lactic acid is inadequately removed from the tissue, causing a decreased pH in the

extracellular matrix of the cancer cell. The second way in which extracellular pH is reduced occurs through carbonic acid buffering by carbon dioxide production. This hypercapnia effect is especially prevalent in combination with poor blood flow to cancerous tissues. The pH gradient between cancerous tissue and normal tissue provides a strong rationale behind the design and efficiency of therapeutics as a function of cellular pH. A challenging aspect of this evaluation is the development and functionality of therapeutics, along with the impending need for them to be non-cytotoxic to the cellular tissue around the tumor site. One such method to take advantage of the extracellular difference in pH between healthy cells and tumor cells would be to encapsulate the therapeutic in a polymer casing.

Polymers, a most versatile class of materials, can be found nearly everywhere from cars to food, polymers have changed our day-to-day lives over the past several decades. However, the convergence of polymer science with pharmaceutical science has only come to fruition over the last several years.[5] Polymers are ideal in biological applications since they are flexible in their physical states, size, shape, and surface.[5] The major role of polymers in biotechnology are as novel therapeutic delivery systems. The idea behind this system is as a means of providing controlled release of therapeutic to a specific site over a certain period of time. Biodegradable polymer drug delivery systems have many advantages over conventional delivery systems. These advantages include localized delivery, avoidance of peaks and valleys in the concentration of the therapeutic delivered, protection of the therapeutic being delivered, and improved drug efficacy. Several different examples of polymer degradation in drug delivery systems are: bulk erosion, surface erosion, hydration, or solubilization. The main focus of this thesis will be on hydration of the polymer backbone. These biodegradable polymers have labile groups built into the polymer

backbone, which make it possible for hydrolysis to occur. These groups include: esters, orthoesters, anhydrides, amides, carbamates, carbonates, urethane, and urea.[6] The rates at which these groups hydrolysis is as follows: polycarbonates > polyesters > polyurethanes > polyorthoesters > polyamides > polyamines.[6] The reason for the increased rate of hydrolysis in polyesters and polycarbonates as opposed to polyamines and polyamides can be seen in the figure below.

Polyamine Polyester

Figure 1: Schematic of polyamine hydrolysis vs. polyester hydrolysis.

In polyamines the electron density in the lone pair of electrons on nitrogen can be donated into the carbon atom forming a partial negative charge on the carbon. This partial negative charge acts like a shield toward nucleophilic water molecules. On the other hand when looking at the bonding in polyesters, the highly electronegative oxygen's pull electron density away from the carbon atom. This in turn forms a partial positive charge on the carbon atom. Since the carbon atom now has a partial positive charge it is more receptive towards nucleophilic attack.

The guide above is only an approximation. Polymer morphology and other adjacent substituent groups can greatly influence the rate of hydrolysis. A variety of biodegradable

polymers have been synthesized for drug delivery. Some of the early examples include poly(lactic acid) (PLA), poly(glycolic acid) (PGA), and poly(lactic acid-co-glycolic acid) (PLGA).[7] Most recently cationic polymers such as poly(ethylene imine) (PEI)[7] and poly(lysine)[8] have been used to mediate transfection to a variety of different cell lines. The problem with using PEI and poly(lysine) is both polymers are extremely cytotoxic, meaning they are not viable as an adequate delivery vector. Another drawback to using these polymers is their expanded synthesis. Present syntheses of these polymers require either the independent preparation of specialized monomers[9] or the use of stoichiometric amounts of expensive coupling reagents. Additionally, the amine functionalities in the monomers must be protected prior to polymerization,[10] necessitating additional post polymerization deprotection steps before the polymers can be used as transfection agent.[11] Two of the major factors which must be considered in developing new polymeric therapeutic delivery vectors are ease of synthesis and maintenance of the hydrolysable backbone. Many of the polymeric delivery vectors previously studied took many long hours of multiple step synthesis work.[10] These new polymeric delivery vectors would be able to be synthesized in a short period of time and include only one or two steps.

The other major factor affecting the development of new polymeric delivery vectors is maintenance of the hydrolysable polymer backbone. This hydrolysable back is the major reason why these polymers are able to do what they do. Without this special chemical composition, the polymer would be unable to open-up and hence be ineffective in releasing the therapeutic.

The idea behind this thesis was to generate a library of different hydrolysable polymers, form fluorescently loaded polymer microsperes out of these polymers by

encapsulating rhodamine-β conjugated BSA, and test their backbone hydrolysability compared to poly(1,4 butanediol diacrylate-co-trimethylene dipiperidine).[11] The polymer spheres discussed in this thesis did meet the two major requirements in developing new polymeric delivery vectors discussed in the previous paragraph. These new polymers contain the hydrolysable backbone needed to maintain the polymers unique release properties, meaning the polymer shell has been specifically designed to degrade and release encapsulate in a low pH tumor environment while maintaining shell integrity in the increased healthy cellular pH environment. On average it does take longer to synthesis these new polymers, but most of that time is reaction time and not laborious synthesis work. Infact most of theses new polymers can be synthesized in only one or two steps.

Chapter 2

Synthesis of linear poly(amido amines) and poly(amino esters) containing tertiary amines in their backbone have been reported by Ferruti, et al[12] in 1970 and most recently by Langer, et al.[11] in 1999. These polymers are synthesized by the addition of bifunctional amines to bisacrylamides and diacrylates. The poly(ester amine) and poly(amino amide) approach to new polymeric transfection vectors is a very attractive platform for several reasons: (1) the polymers contain the requisite amines and readily degradable linkages, (2) multiple analogues can be synthesized directly from commercially available starting materials, (3) preliminary studies show these polymers to be less cytotoxic than previous polymer transfection vectors.[11] The synthesis of these new polymers occurs via a 1,4 conjugate addition mechanism, also known as the Michael reaction.[12] In this reaction primary and secondary amines add to chemically activated double bonds at the expense of an unshared electron pair at the Nitrogen atom.[13] The general reaction scheme of the Michael reaction is shown below in figure 2.

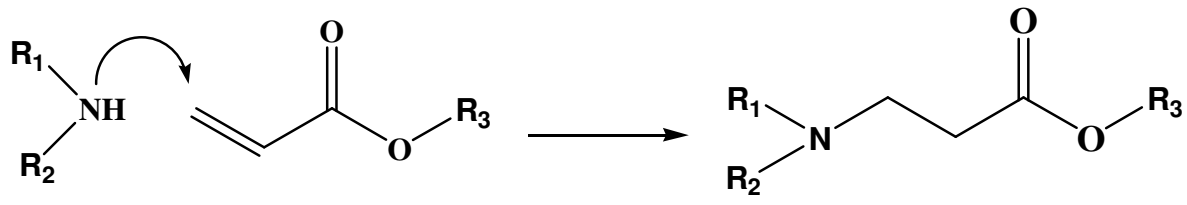

Figure 2: General scheme of a Michael addition.

The general polymerization procedure for the polymers studied in this thesis are as follows: In a typical experiment, 3.70mmol of diacrylate or methylene bisacrylamide and 3.70mmols of diamine were weighed into two separate vials and dissolved in 5ml each of dry dichloromethane. The solution containing the diamine was added to the diacrylate solution via pipette. A Teflon-coated stirbar was added, the vial was sealed with a Teflon-lined screw-cap, and the reaction was heated at 50 °C. After 72h, the reaction was cooled to room temperature and purified by repeated precipitations from slowly dripping polymer solution into vigorously stirring diethyl ether or hexanes. Both diethyl ether and hexanes where used in precipitation of each polymer. Using hexanes showed a slight increase in polymer yield, but was not significant enough to require specific use. Polymer was collected on filter paper using vacuum filtration and dried under vacuum prior to analysis. The polymers synthesized in this thesis are as follows: Poly(1,3-butanediol diacrylate-co-2-aminoethanol), Poly(1,4-butanediol diacrylate-co-2-aminoethanol), Poly(N,N-methylene bisacrlyamide-co-2-aminoethanol), Poly(1,3-butanediol diacrylate-co-trimethylene dipiperidine), Poly(1,4-butanediol diacrylate-co-trimethylene dipiperidine), Poly(N,N-methylene bisacryamide-co-trimethylene dipiperidine), Poly(1,3-butandiol diacrylate-co-benzyl amine), and Poly(1,4-butandiol diacrylate-co-benzyl amine): [Amounts of monomer used, polymer yield, structure, molecular weight (calculated from ^{1}HNMR), and characterizations (^{1}HNMR and ^{13}CNMR Gemini 300Mhz) are located in the appendix of thesis]

Chapter 3

Microencapsulation of water-soluble biological materials has been widely studied.[14] The encapsulation of water-soluble therapeutic compounds within tiny polymer microspheres is often achieved via a double emulsion process.[15] In this process, the polymer is dissolved in a water immiscible solvent, and the therapeutic is dispersed or dissolved in the polymeric solution. The resultant solution is then emulsified in a continuous aqueous phase to form discrete droplets. Formation of the microspheres occurs as the organic solvent diffuses into the aqueous phase and then evaporates at the air/water interface. As solvent evaporation occurs, the newly formed microspheres harden, and can be obtained after filtration and suitable drying.[14] Sizes of microspheres formed via a double emulsion can be altered in several different ways. When the amount of solvent used to dissolve the polymer was increased, the size of the microspheres formed decreased. Also, as the concentration of dispersing agent increased the size of microspheres formed decreased. Finally, as the rate of homogenization was increased the size of formed microspheres decreased.[14]

For the purposes of testing hydrolysis rates of the polymers synthesized earlier, rhodamine β-conjugated bovine serum albumin (RB-BSA) was chosen as the encapsulate. The BSA protein was chosen for its biocompatibility and physical characteristics. Rhodamine β was chosen as a label for two reasons: (1) rhodamine is fluorescent, thus allowing for release profiles to be determined by fluorescence spectroscopy. (2) fluorescence intensity of rhodamine is relatively unaffected by pH values within the physiological range.[16] The experimental details for the encapsulation of RB-BSA are as follows. An aqueous solution of rhodamine β-conjugated BSA (200mL of a 10mg/ml) was suspended in a solution

of polymer in CH_2Cl_2 (200mg of polymer in 4mL of CH_2Cl_2). This mixture was sonicated for 10 seconds to form a primary emulsion. The cloudy pink emulsion was added directly to a rapidly homogenized (5000 rpm) solution of poly(vinyl alcohol) (50mL, 1% PVA (w/w)) to form the secondary emulsion. The secondary emulsion was homogenized for 30 seconds before adding it to a second aqueous PVA solution (100mL, 0.5% PVA (w/w). The secondary emulsion was stirred for 2.5 hours at room temperature before being transferred to a cold room (48^{o}C), and stirred for an additional 30 minutes. The microspheres were isolated at 48^{o}C by centrifugation, resuspended in cold water, and centrifuged again to remove excess PVA. The spheres were resuspended in water (15mL) and lyophilized to yield a pink, fluffy powder. Characterization of the lyophilized microspheres was performed by scanning electron microscopy. Images of the isolated polymer microspheres are shown in figures 3 and 4 below.

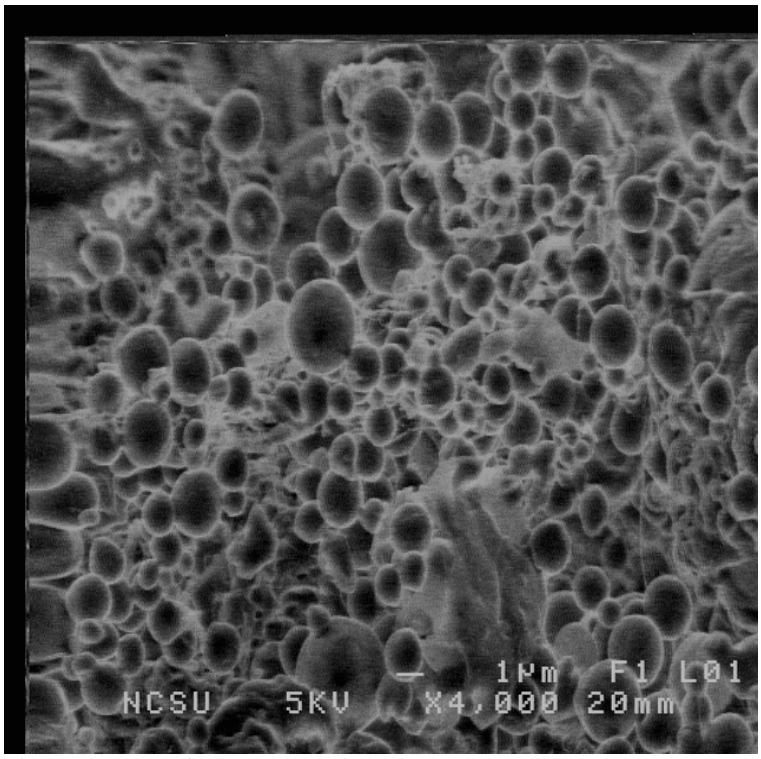

Figure 3: SEM of RB-BSA loaded microspheres cluster.

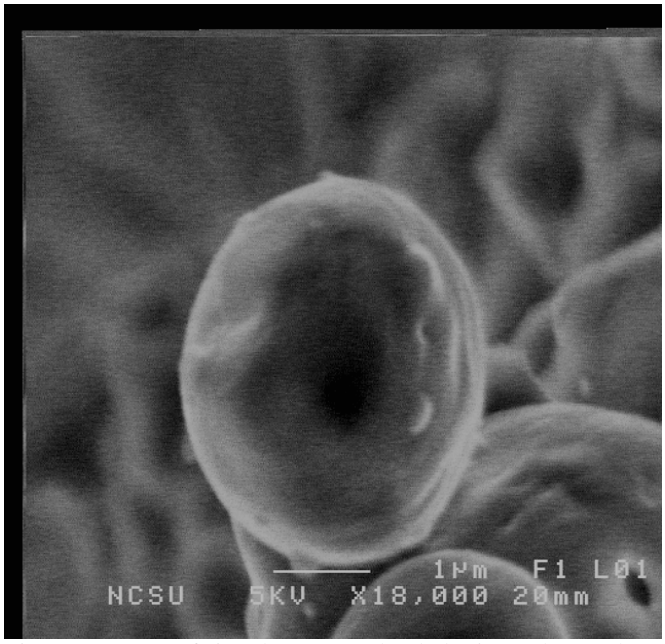

Figure 4: SEM of signal RB-BSA loaded microspheres cluster.

Chapter 4

Polymer release profiles were generated for a majority of the polymers synthesized above. The idea behind this thesis was to generate a library of different hydrolysable polymer microspheres and test their polymer backbone degradation compared to poly(1,4 butanediol diacrylate-co-trimethylene dipiperidine).[11] Poly(1,4BDDA-co-TMDP) was chosen as the primary reference material because its release profile has previously been reported by Langer, et al.[11] Poly(1,4BDDA-co-TMDP) is the only polymer in the study which has been previously synthesized.[11] The release profiles are based on the measured fluorescence of rhodamine β–conjugated bovine serum albumin (BSA) released from polymer microspheres formed using the various polymers and techniques previously mentioned. The profiles were generated after six hours of exposure to acetic acid buffered solutions ranging in pH from 5.5-7.4 pH units. Six hour exposure to 0.1M HCl was set as the standard for 100% release (hydrolysis) since the pH of a 0.1M solution of HCl is 1.0. If the polymer microsphere backbone would not hydrolysis in a 0.1M solution of HCl, the polymer was not going to hydrolyze. The percentage of release was calculated by finding the area under each spectral curve for a given pH, then dividing that area by the total area under the spectral curve for each rhodamine β–conjugated BSA loaded polymer microsphere in the 0.1M solution of HCl. Blank spectra of BSA where taken at each pH level and subtracted from the total area of the release profiles. This was done to ensure only the fluorescence of the rhodamine was being measured and there was not a problem with the molecular conformation of BSA in varying pH buffers. The chart below shows the percentage of release from each polymer in the corresponding pH, table 1.

	pH of Buffer Solution				
Polymers	**5.5**	**6**	**6.5**	**6.8**	**7.4**
Poly(1,4-BDDA-co-TMDP)	69%	63%	48%	32%	9%
Poly(1,4-BDDA-co-2-AE)	64%	52%	17%	5%	3%
Poly(1,3-BDDA-co-BA)	No relevant Release at Physiological pH				
Poly(1,3-BDDA-co-TMDP)	66%	61%	45%	17%	6%
Poly(1,4-BDDA-co-BA)	No relevant Release at Physiological pH				
Poly(MBAA-co-TMDP)	84%	81%	78%	39%	<1%

Table 1: Release percentages of RB-BSA from polymer microspheres.

There are several interesting conclusions which can be drawn regarding the polymer backbone characteristics. These conclusions were drawn by looking at the measured fluorescence from rhodamine β-conjugated BSA released when a polymer microsphere is hydrolyzed.

First, the polymers synthesized from primary amines showed a greater resistance towards hydrolysis. This observation was not surprising since Michael type reactions of primary amines are favored over secondary amines. Another reason for this resistance towards hydrolysis can be explained by looking at the structure of the polymer backbone. All of the polymers formed from primary amines had side chains extending away from the polymer backbone. This side chain, due to its bulky steric hindrance could also inhibit hydrolysis of the polymer backbone. This was seen in the release profiles for poly(1,4-BDDA-co-2-AE) and poly(1,4-BDDA-co-BA) when compared with the release profiles for poly(1,4-BDDA-co-TMDP), figures 5 and 6.(No release profile is shown for poly(1,4-BDDA-co-BA since it showed no release in the pH range tested) Poly(1,4-BDDA-co-TMDP) showed the highest percentage of rhodamine β-conjugated BSA release when compared to other polymers containing the same 1,4 butanediol diacrylate monomer, but different primary amines as the other monomer.

Another major factor affecting polymer backbone hydrolysis was the size of the substituent group located in either the alpha position next to the carbonyl or directly coming off of the reactive amine. As shown in table 1, when comparing primary amines, poly(1,4-BDDA-co-2-AE) showed a greater percentage of rhodamine β-conjugated BSA released from the polymer sphere when compared to poly(1,4-BDDA-co-BA), figures 5 and 6.

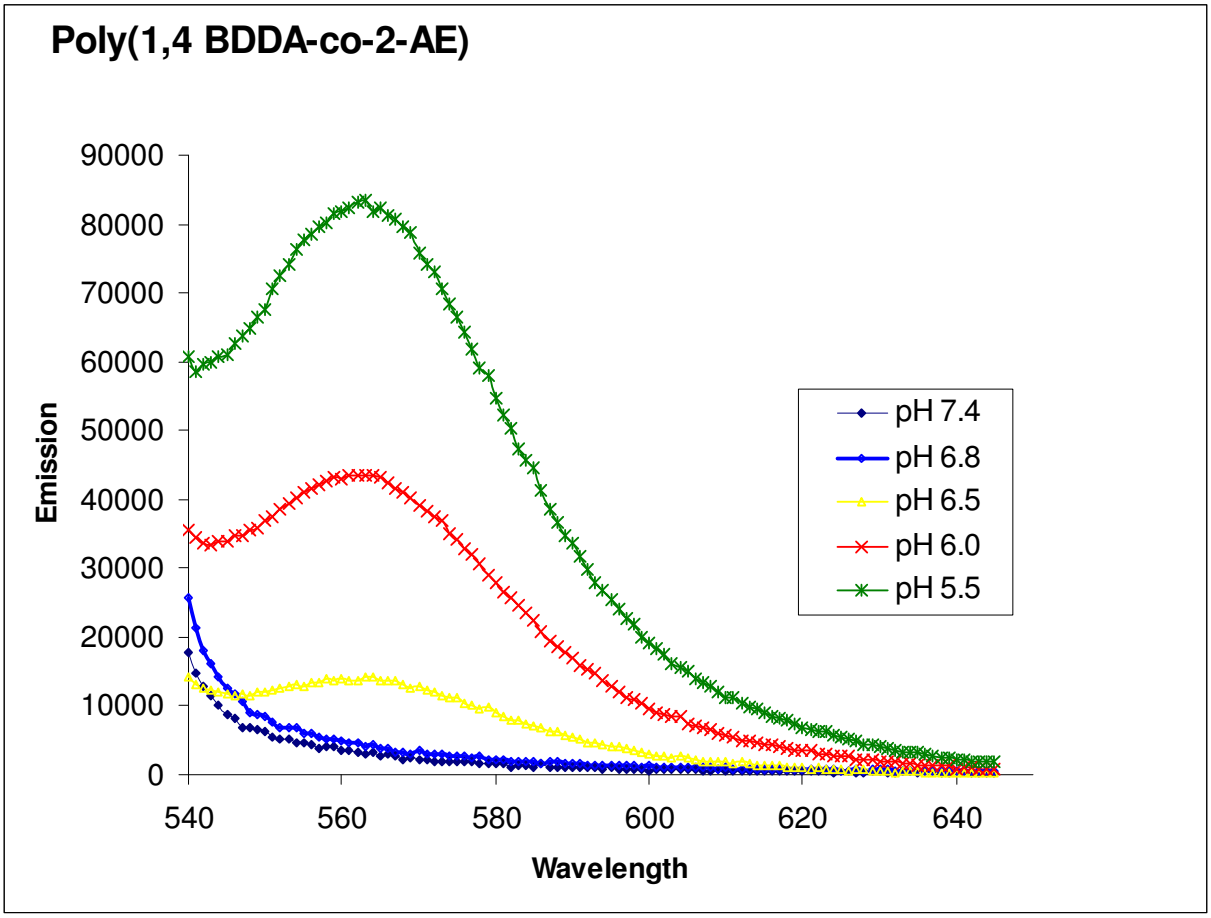

Figure 5: Fluorescence release profile of poly(1,4 BDDA-co-2-AE) polymer microsphere containing rhodamine β-conjugated BSA.

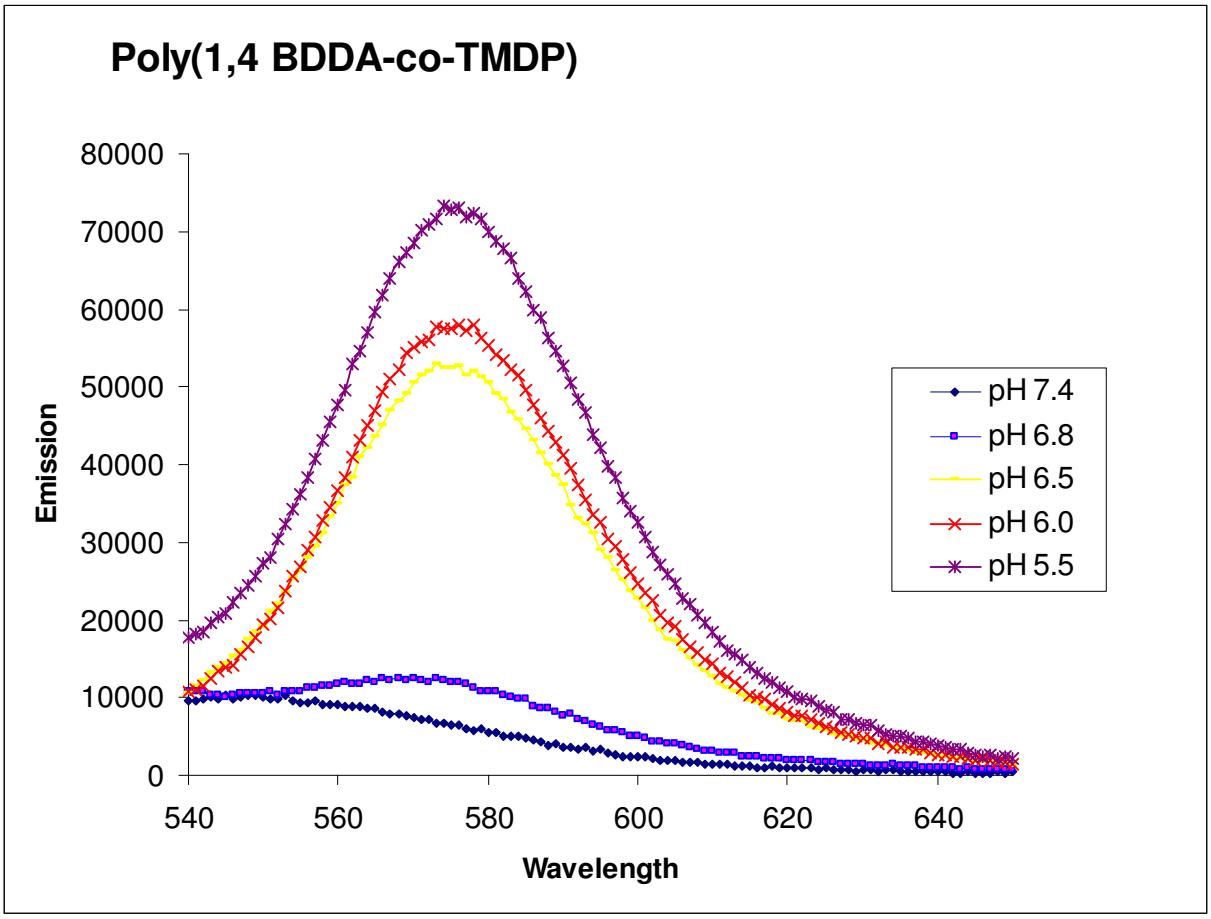

Figure 6: Fluorescence release profile of poly(1,4 BDDA-co-TMDP) polymer microsphere containing rhodamine β-conjugated BSA

As table one shows, poly(MBAA-co-TMDP) has the highest percentage of labeled BSA release from pH 6.8 which is the approximate extracellular pH of cancerous tumor cells. Poly(MBAA-co-TMDP) also has the lowest percentage of release at pH 7.4 when compared to the other polymers in the study, figure 7.

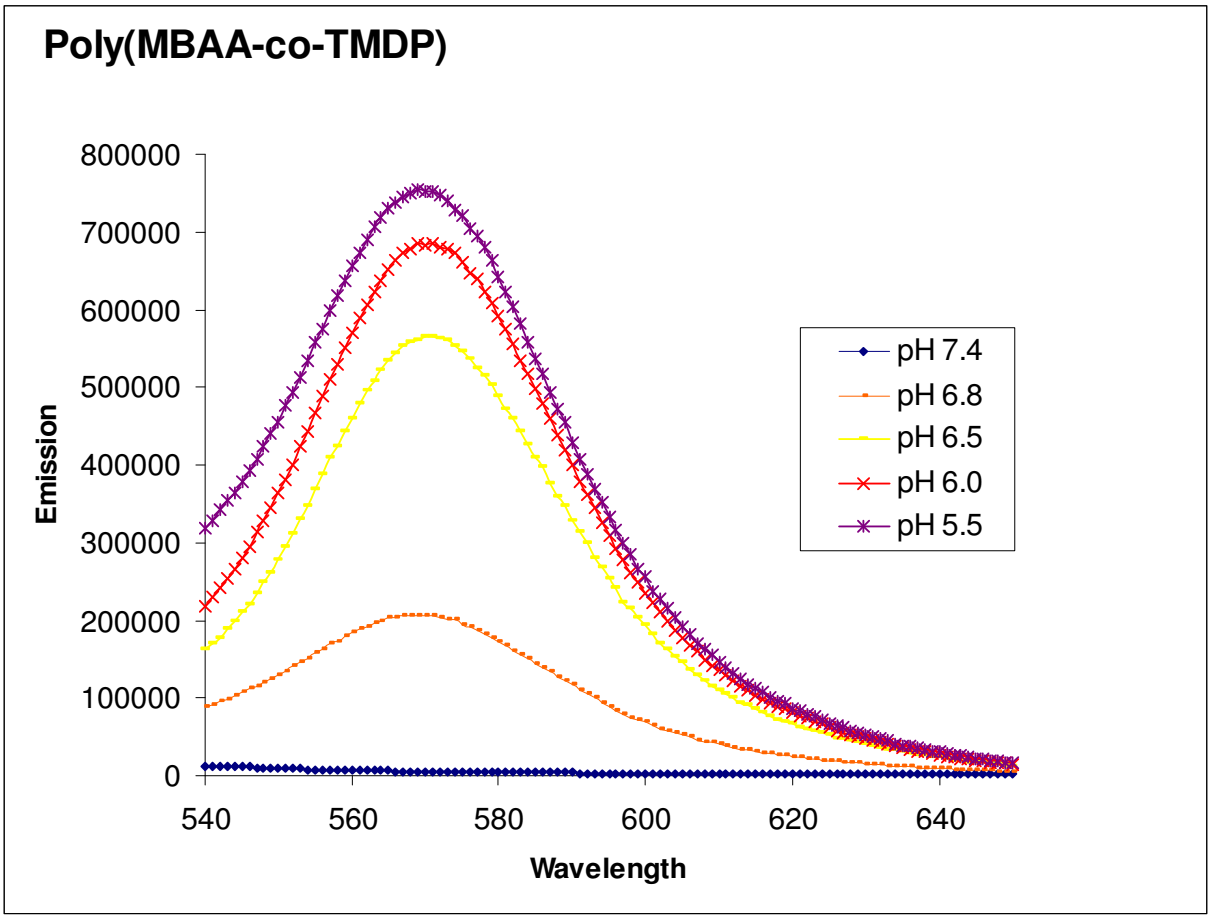

Figure 7: Fluorescence release profile of poly(1,4 MBAA-co-TMDP) polymer microsphere containing rhodamine β-conjugated BSA

To test poly(MBAA-co-TMDP) as a viable alternative to Langer's poly(1,4-BDDA-co-TMDP) over an extended period of time, a six day release profile was calculated, tables 2 and 3.

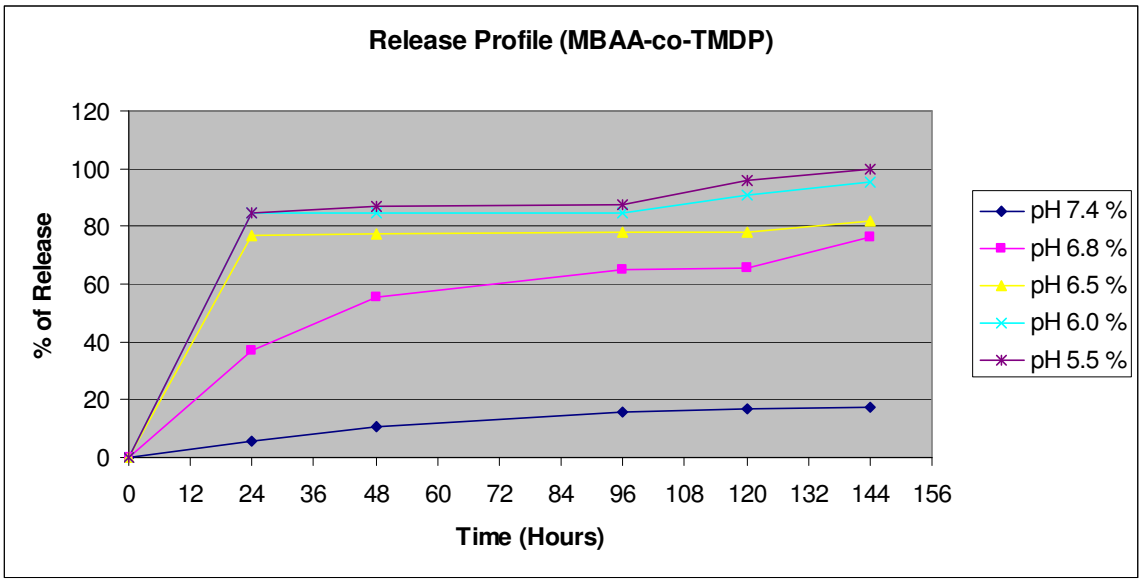

Table 2: Six day release profile of poly(MBAA-co-TMDP)

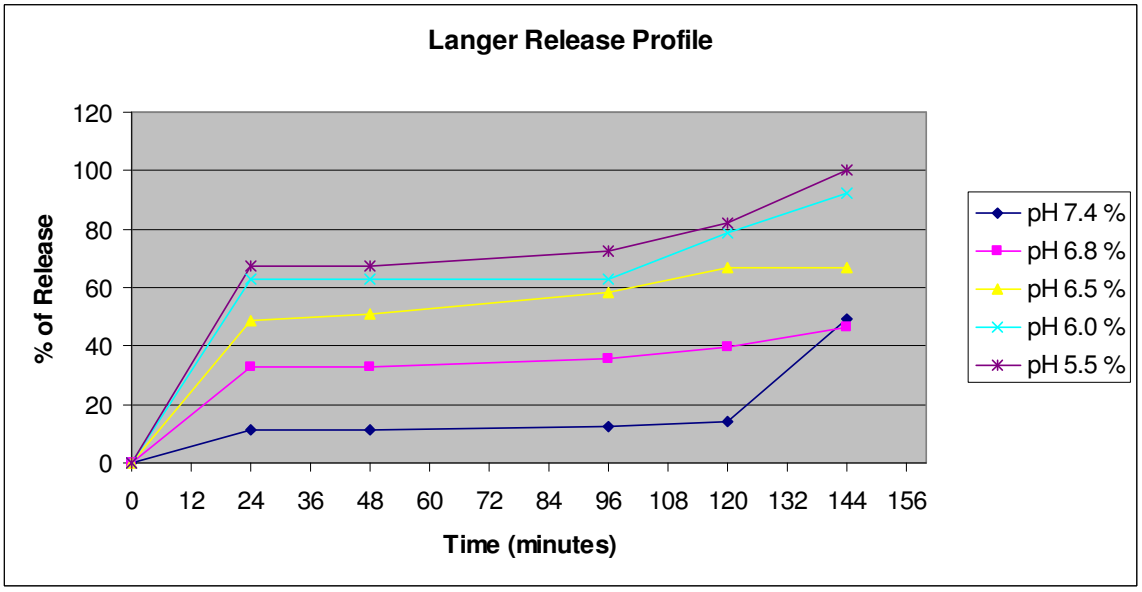

Table 3: Release profile of poly(1,4-BDDA-co-TMDP)

As the release profiles show, poly(MBAA-co-TMDP) offers a greater percentage of release over all pHs except pH 7.4. This is very important since the idea behind the project is to create a polymer which maximizes release at pH 6.8 and minimizes release at pH 7.4. The

lower release at pH 7.4 for poly(MBAA-co-TMDP) against poly(1,4-BDDA-co-TMDP) makes sense since esters are more reactive towards hydrolysis than amides. However, the increased release at pH 6.8 was somewhat surprising.

Something else which was somewhat surprising is the large increase in percentage of fluorescence of rhodamine β-conjugated BSA released between the fifth and sixth day in Dr. Langers polymer. The experiment was performed several times with the same result. One explanation might be the polymers reach a maximum hydrolyzed state after being in the buffers for five days. After this point the polymer is completely hydrolyzed achieving maximum release. The problem with this explanation is if the polymer reaches maximum release, then the measured percentage of release between day five and six would jump all the way to 100 percent. It does not! The explanation could be after day five the rate of the polymer hydrolysis is increased and more rhodamine β-conjugated BSA is released from the polymer microsphere.

Chapter 5

Polymer science has been the backbone for the development of new therapeutic delivery systems over the past several decades. This thesis has hopefully shed some light on two new classes of polymers for use as potential therapeutic delivery vectors. Both poly(β−amino esters) and poly(β−amino amides) posses many of the key characteristics needed for a therapeutic delivery system. These therapeutic delivery systems are certainly not the benchmark and may never make it to market. However, they do offer a good initial starting point for which further modification may be made to the polymer backbone, which someday could make site specific cell targeting a reality.

References:

1. Gerweck, Leo E. and Seetharaman, K. *Cancer Research,* **1996**, 56, 1194-1198.

2. Montcourier, P., Silver, I., Farnoud, R., Bird, I. and Rochefort, H. *Metastasis*, **1997**, 15, 382-392.

3. Montcourier, P., Mangeat, P.H., Valembois, C., Salazar, G., Sahuquet, A., Duperray, C. *J. Cell Science*, **1994**, 107, 2381-2391.

4. Martin, G. and Rakesh, J.K. *Cancer Research*, **1994**, 54, 5670-5674.

5. Pillai, O. and Panchagnula, R. *Current Opinion in Chemical Biology*, **2001**, 5, 447-451.

6. Gombotz, W. and Pettit, D. *Bioconjugate Chemistry*, **1995**, 6, 332-351.

7. Boussif, O.; Lezoualc'H., F.; Zanta, M. A.; Mergny, M. D.; Scherman, D.; Demeneix, B.; Behr, J. P. *Proc. Natl. Acad. Sci. U.S.A.* **1995**, *92*, 7297-7301.

8. Zauner, W.; Ogris, M.; Wagner, E. *Ad*V. *Drug Del. Re*V. **1998**, *30*, 97-113.

9. Lim, Y.-B.; Kim, C.-H.; Kim, K.; Kim, S. W.; Park, J.-S. *J. Am. Chem. Soc.* **2000**, *122*, 6524-6525.

10. Putnam, D.; Langer, R. *Macromolecules* **1999**, *32*, 3658-3662.

11. Lynn, D.M., Langer, R. *J. Am. Chem. Soc.* **2000,** *122,* 10761-10768

12. Danusso, F.; Ferruti, P. *Polymer* **1970**, *11*, 88-113.

13. Kargina, O.V., Mishustina, L.A., Kiselev, V.Ya., Kabanov, V.A. *Polymer Science U.S.S.R.* **1986**, 28, 1265-1272.

14. O'Donnell, P.B., and McGinity, J.W. *Advanced Drug Delivery*. **1997**, 28, 25-42.

15. Lynn, D.M., Amiji, M.M., Langer, R. *Angew. Chem. Int. Ed.* **2001**, 40, 1707-1710.

16. Haugland, R.P. *Handbook of Fluorescent Probes and Research Chemicals, 6th ed.* **1996**, 29.

Appendices

Poly(1,3-butanediol diacrylate-co-2-aminoethanol) Used 0.7530g (0.7310ml) of 1,3-BDDA and 0.2276ml of 2-aminoethanol. Polymer yield was 76%. Proton NMR showed: δ 4.10(br, m), 3.24(br,t), 2.75(br,t), 2.49(br,t), 2.39(br,t), 1.84(br, d), 1.62(br, t). Carbon NMR showed: δ 172.46, 68.20, 63.55, 61.09, 59.44, 34.95, 32.34, 24.41.

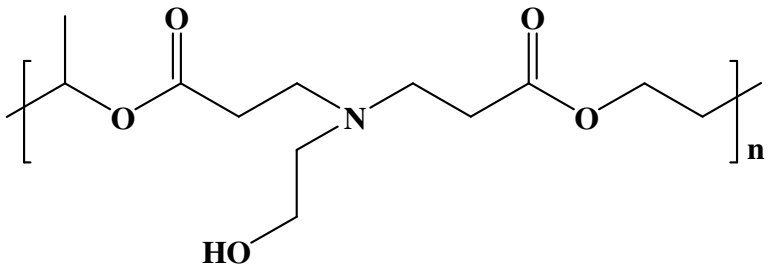

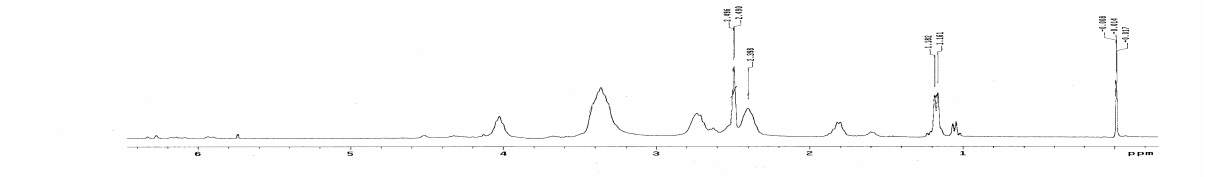

Figures 8 (top) and 9 (bottom): Structure of Poly(1,3-butanediol diacrylate-co-2-aminoethanol) (figure 8), ^{1}H NMR of Poly(1,3-butanediol diacrylate-co-2-aminoethanol) (figure 9)

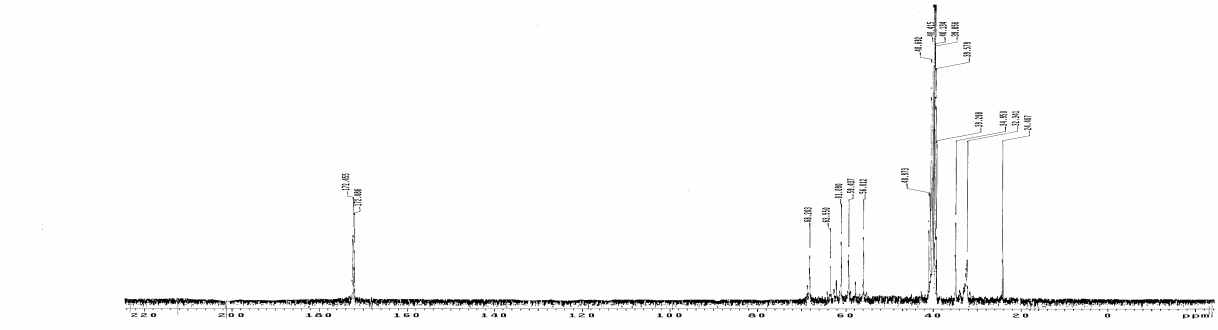

Figure 10: ^{13}C NMR of Poly(1,3-butanediol diacrylate-co-2-aminoethanol)

Poly(1,4-butanediol diacrylate-co-2-aminoethanol) Used 0.7530g (0.7140ml) of 1,4-BDDA and 0.2276ml of 2-aminoethanol. Polymer yield was 73%. Proton NMR showed: δ 4.10(br, t), 3.64(br, t), 2.80(br, t), 2.63(br, t), 2.47(br, t), 1.65(br, t). Carbon NMR showed: δ 172.77, 64.27, 62.58, 59.20, 55.96, 32.60, 25.27.

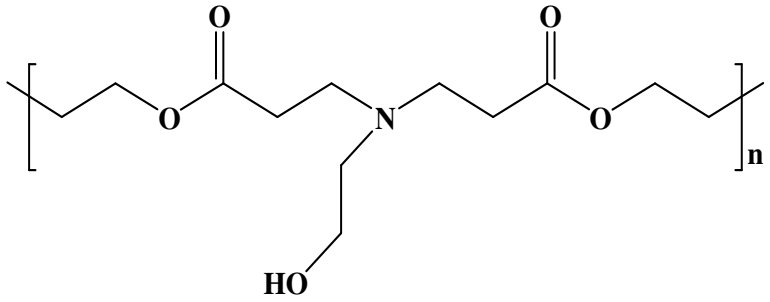

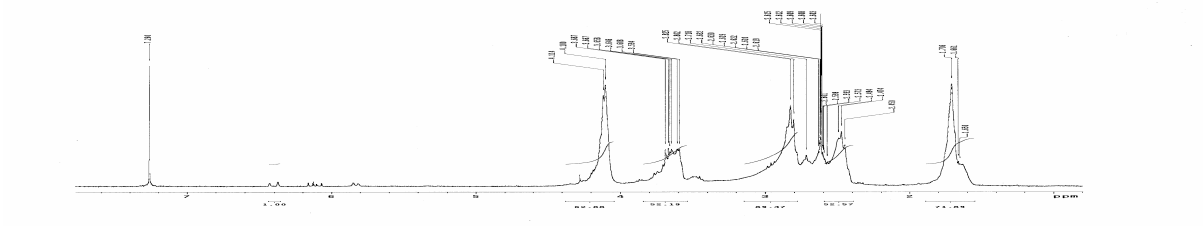

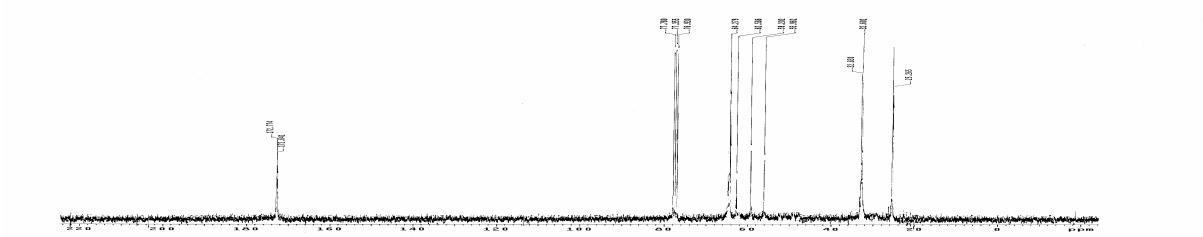

Figures 11 (top), 12 (middle), and 13 (Bottom): Structure of Poly(1,4-butanediol diacrylate-co-2-aminoethanol) (figure 11), ^{1}H NMR of Poly(1,4-butanediol diacrylate-co-2-aminoethanol) (figure 12), and ^{13}C NMR of Poly(1,4-butanediol diacrylate-co-2-aminoethanol) (figure 13)

Poly(N,N-methylene bisacrlyamide-co-2-aminoethanol) Used 0.5860g of N,N-MBAA and 0.2276ml of 2-aminoethanol. Polymer yield was 81%. Proton NMR showed: δ 8.51(br, t), 4.35(br, t), 3.38(br, t), 2.64(br, t), 2.43(br, t), 2.18(br, t). Carbon NMR showed: δ 173.12, 58.66, 55.89, 50.23, 33.56.

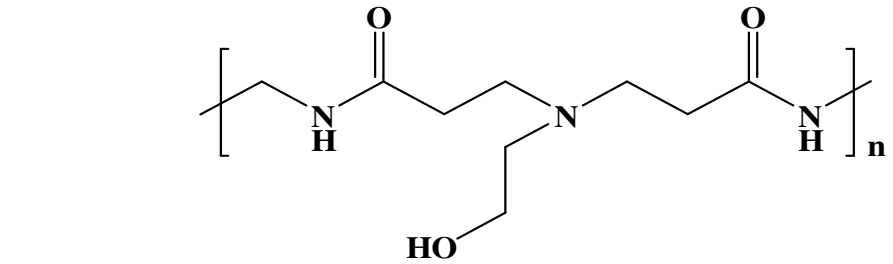

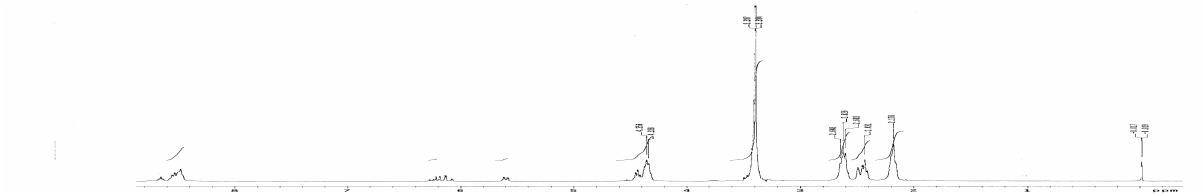

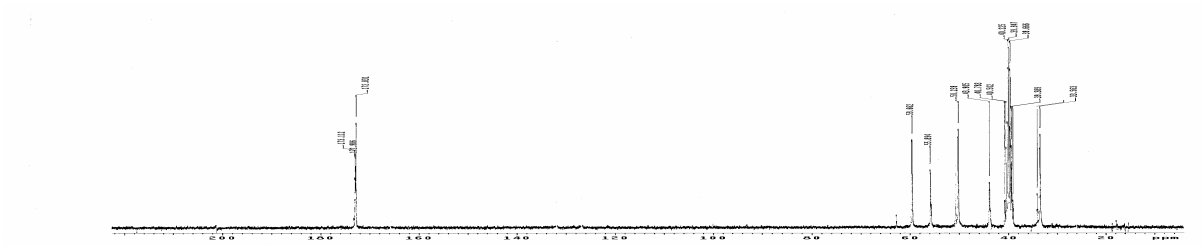

Figures 14 (top), 15 (middle), and 16 (Bottom): Structure of Poly(N,N-methylene bisacrlyamide-co-2-aminoethanol) (figure 14), ^{1}H NMR of Poly(N,N-methylene bisacrlyamide-co-2-aminoethanol) (figure 15), and ^{13}C NMR of Poly(N,N-methylene bisacrlyamide-co-2-aminoethanol) (figure 16)

Poly(1,3-butanediol diacrylate-co-trimethylene dipiperidine) Used 0.7530g (0.7310ml) of 1,3-BDDA and 0.7990g of TMDP. Polymer yield was 54%. Proton NMR showed: δ 3.85(br, t), 2.79(br, t), 2.57(br, t), 2.39(br,t), 1.81(br, t), 1.72(br, t), 1.46(br, m), 1.07(br, m).

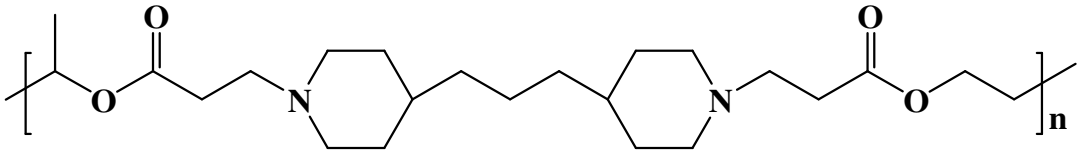

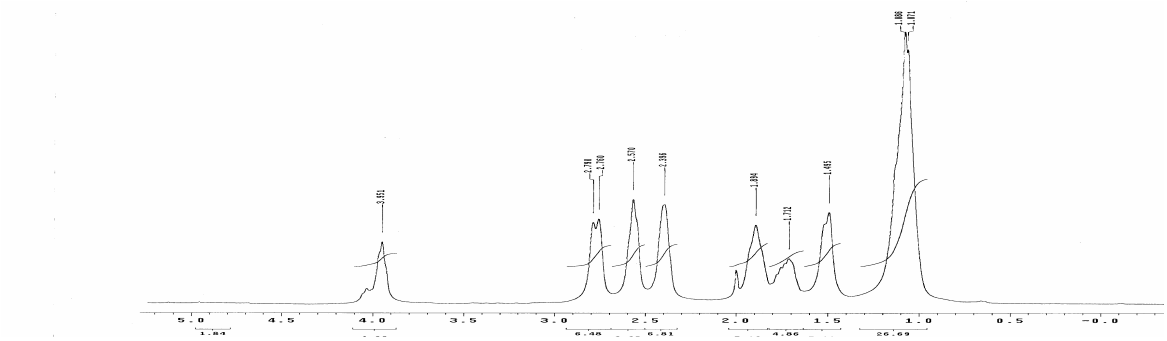

Figures 17 (top) and 18 (bottom): Structure of Poly(1,3-butanediol diacrylate-co-trimethylene dipiperidine) (figure 17), ^{1}H NMR of Poly(1,3-butanediol diacrylate-co-trimethylene dipiperidine) (figure 18)

Poly(1,4-butanediol diacrylate-co-trimethylene dipiperidine) Used 0.7530g (0.7140ml) of 1,4-BDDA and 0.7990g of TMDP. Polymer yield was 79%. Proton NMR showed: δ 3.97(br, t), 2.84(br, t), 2.65(br, t), 2.48(br, t), 2.02(br, t), 1.89(br, m), 1.58(br, m), 1.15(br, m).Carbon NMR showed: δ 172.24, 68.31, 61.03, 53.63, 36.49, 35.28, 34.91, 31.70, 25.33, 23.85, 20.18.

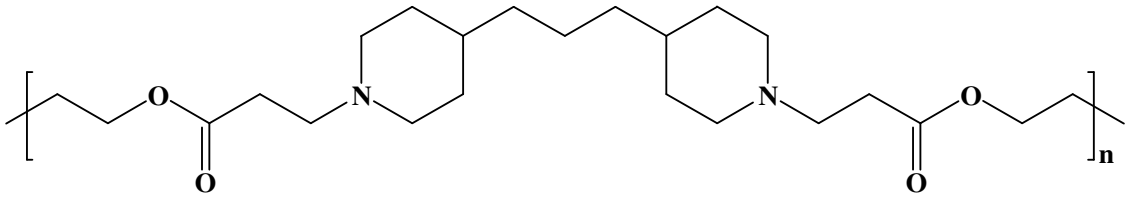

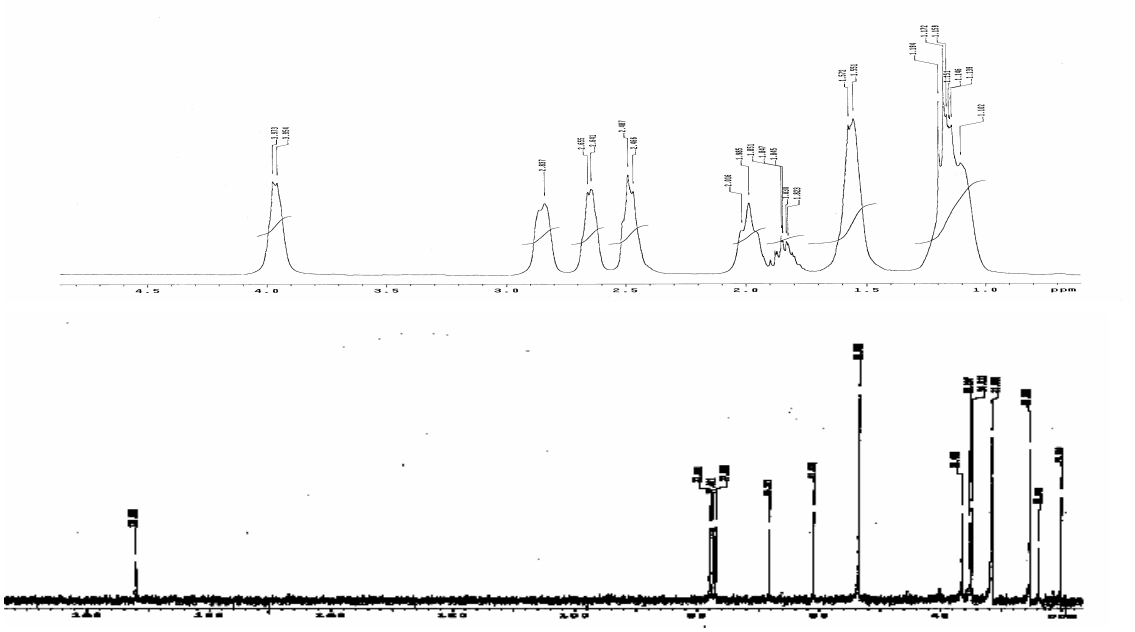

Figures 19 (top), 20 (middle), and 21 (Bottom): Structure of Poly(1,4-butanediol diacrylate-co-trimethylene dipiperidine) (figure 19), ^{1}H NMR of Poly(1,4-butanediol diacrylate-co-trimethylene dipiperidine) (figure 20), and ^{13}C NMR of Poly(1,4-butanediol diacrylate-co-trimethylene dipiperidine) (figure 21)

Poly(N,N-methylene bisacryamide-co-trimethylene dipiperidine) Used 0.5860g of N,N-MBAA and 0.7990g of TMDP. Polymer yield was 73%. Proton NMR showed: δ 8.91(br, t), 4.69(br, t), 4.56(br, t), 2.90(br, t), 2.54(br, t), 2.34(br, t) 1.93-1.64(br, m), 1.23(br, m).

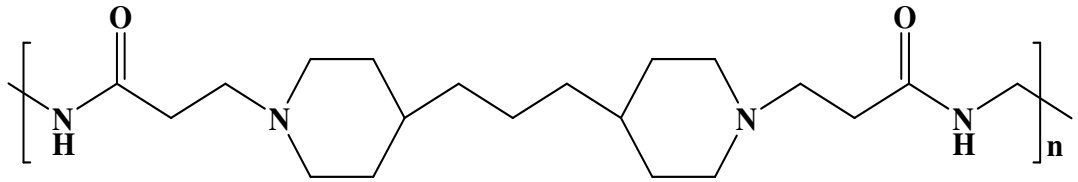

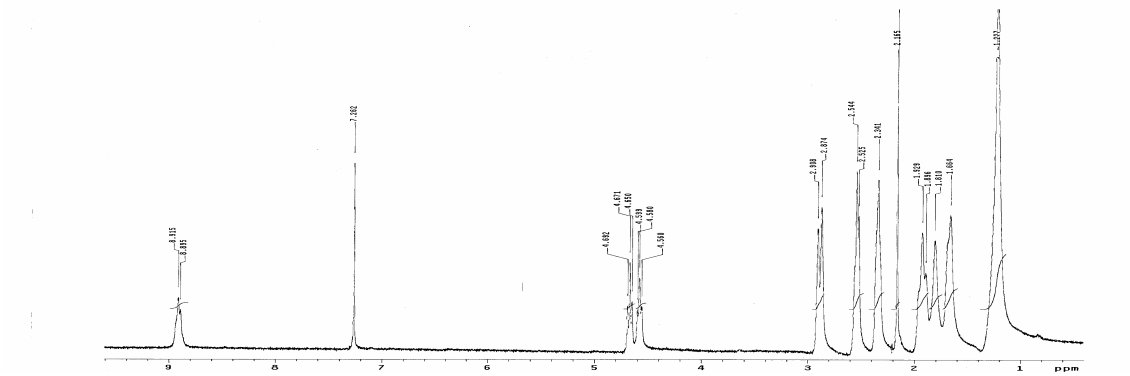

Figures 22 (top) and 23 (bottom): Structure of Poly(N,N-methylene bisacryamide-co-trimethylene dipiperidine) (figure 22), ^{1}H NMR of Poly(N,N-methylene bisacryamide-co-trimethylene dipiperidine) (figure 23)

Poly(1,3-butandiol diacrylate-co-benzyl amine) Used 0.7530g (0.7310ml) of 1,3-BDDA and 0.4040ml of BA. Polymer yield was 56%. Proton NMR showed: δ 7.32-7.21(br, m), 3.96(br, t), 3.50(br, s), 3.33(br, d), 2.63(br, t), 2.47(br, t), 1.84(br, d), 1.14(br, t). Carbon NMR showed: δ 172.39, 139.85, 129.46, 127.74, 68.14, 57.84, 34.92, 20.14.

Figures 24 (top), 25 (middle), and 26 (Bottom): Structure of Poly(1,3-butanediol diacrylate-co-benzyl amine) (figure 24), ^{1}H NMR of Poly(1,3-butanediol diacrylate-co-benzyl amine) (figure 25), and ^{13}C NMR of Poly(1,4-butanediol diacrylate-co-benzyl amine) (figure 26)

Poly(1,4-butandiol diacrylate-co-benzyl amine) Used 0.7530g (0.7140ml) of 1,4-BDDA and 0.4040ml of BA. Polymer yield was 54%. Proton NMR showed: δ 7.32-7.21(br, m) 4.00(br, t) 3.75(br, s) 2.76(br,t) 2.64(br,t) 2.39(br, t) 1.51(br, t). Carbon NMR showed: δ 172.61, 139.85, 129.33, 127.27, 64.12, 57.89, 52.77, 34.38, 25.44.

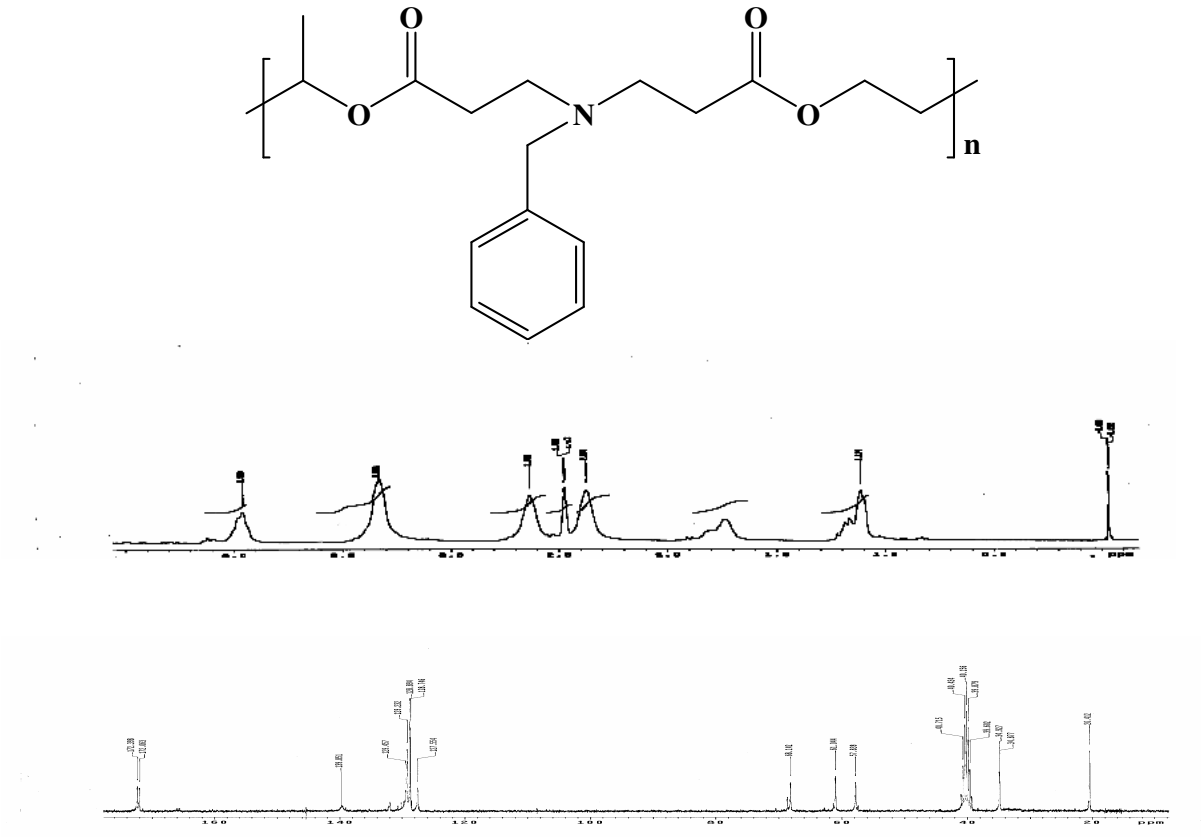

Figures 27 (top), 28 (middle), and 29 (Bottom): Structure of Poly(1,4-butanediol diacrylate-co-benzyl amine) (figure 27), ^{1}H NMR of Poly(1,4-butanediol diacrylate-co-benzyl amine) (figure 28), and ^{13}C NMR of Poly(1,4-butanediol diacrylate-co-benzyl amine) (figure 29)

Abstract

Interest in the preparation, characterization, and properties of self assembled monolayers (SAMs) has grown significantly over the last few years. Poly ethylene glycol (PEG) (HO-$(CH_2CH_2\text{-}O)_n$-H) can be monofunctionalized by replacing one of the terminal hydroxyl groups with the thiol –SH group. The resulting molecule can be readily self-assembled on colloidal gold nanoparticles using a thiotic acid intermediate. This thesis reports the synthesis and characterization of modified polyethylene glycol as a colloidal stabilizer.

Table of Contents

List of Figures……II

List of Tables……III

1. Introduction……...1

2. Synthesis of Mercapto-Polyethylene Glycol……7

3. Formation and CCC Results of Gold-Mercapto-Polyethylene Glycol Conjugates…….....11

4. Conclusion……14

5. References……15

List of Figures

Figure 1 General scheme representing the cellular uptake and nuclear localization of a delivery vector……...2

Figure 2 General representation of receptor mediated-endocytosis, with major steps (arrows) numbered……3

Figure 3 Representations of a nuclear pore complex. Picture a.) is a protein structural model of a nuclear pore complex [taken from Hinshaw, J.E., et al; *Cell* **1992**, *69*, 1133] and b.) is a cross-sectional schematic of a nuclear pore complex embedded in a nuclear envelope……...4

Figure 4 General scheme representing the linking of NLS peptide to BSA, then associating BSA with citrate-coated colloidal gold……....5

Figure 5 Structural reaction scheme of polyethylene glycol into *p*-Tolylsulfonyl polyethylene glycol)……..…8

Figure 6 Structural reaction scheme *p*-Tolylsulfonyl polyethylene glycol) into Bromo-(polyethylene glycol)……..…..9

Figure 7 Structural reaction scheme of Bromo-(polyethylene glycol) into thiolacetate protected polyethylene glycol……..10

Figure 8 Structural reaction scheme of thiolacetate protected polyethylene glycol into mercapto-polyethylene glycol……10

List of Tables

Table 1 Molecular weights and units of starting polyethylene glycol.7

Table 2 Amount of starting materials used and final yields in synthesis of varying length (*p*-Tolylsulfonyl polyethylene glycol)….8

Table 3 Amount of starting materials used and final yields in synthesis of varying length Bromo-(polyethylene glycol)……...8

Table 4 Amount of starting materials used and final yields in synthesis of varying length Mercapto-(polyethylene glycol)**……..9**

Table 5 Critical Coagulation Concentrations of various sizes of Mercapto-(polyethylene glycol) attached to various sizes of gold nanoparticles……...12

Chapter 1

In recent years, there has been considerable interest in the development of vectors capable of delivering molecules of biological significance to the nuclei of eukaryotic cells, with particular regard to drug delivery and gene therapy. Existing research includes the following avenues: polymeric, liposomal, projectile/injection techniques, and viral.[1-8] Although great progress has been made in these fields, each has its limitations. Biodegradable polymer delivery systems are limited by their ability to degrade spontaneously in aqueous environments, leading to potentially inefficient administration of desired molecule(s). Other non-biodegradable polymer systems frequently suffer from toxicity and solubility issues. Current liposomal approaches have been shown to successfully deliver molecules *in vitro* and *in vivo* to the cytoplasm at lower efficiencies, but are often cytotoxic and difficult to modify for delivery purposes. Gene gun or injection delivery approaches are invasive and are not practical for *in vivo* application. Lastly, viral vectors, while potentially very efficient, are limited by their payload capacity (30-100 nm), are problematic to modify, and exhibit a propensity to provoke autoimmune responses, especially at high concentrations.

Methods for using metal nanoparticles as biological probes have been previously studied.[9-12] Gold and silver nanoparticles are commonly used as biological staining reagents, imaging of assorted cellular processes via transmission electron microscopy (TEM), and detecting various biomolecules. Although nanoparticles composed of other substances have recently been used to deliver therapeutic agents to cells, these systems are subject to fluorescence bleaching and "blinking." Consequently, colloidal gold was chosen as a starting point in the interest of developing a novel cellular delivery vector because of its prevalent use

as a diagnostic tool, ease of detection and modification, and the lack of bleaching or blinking problems.

Although targeting other parts of a eukaryotic cell could be possible,[13] the specific aim of investigating this novel delivery vector will be the construction of a vector which efficiently localizes in the nuclei of eukaryotic cell. The nucleus, of course, is where the genetic material of a cell resides, and targeting this location would be highly desirable for probing potential disease diagnoses and examining prospective treatments/therapeutic agents to combat disorders at the cellular level. Generally, it is necessary for any delivery vector to 1.) gain access to cells in a reliable, non-toxic fashion and 2.) capable of entering the nucleus of that cell (Figure 1). An understanding of normal cell processes is needed in order to address these issues in a logical fashion.[14]

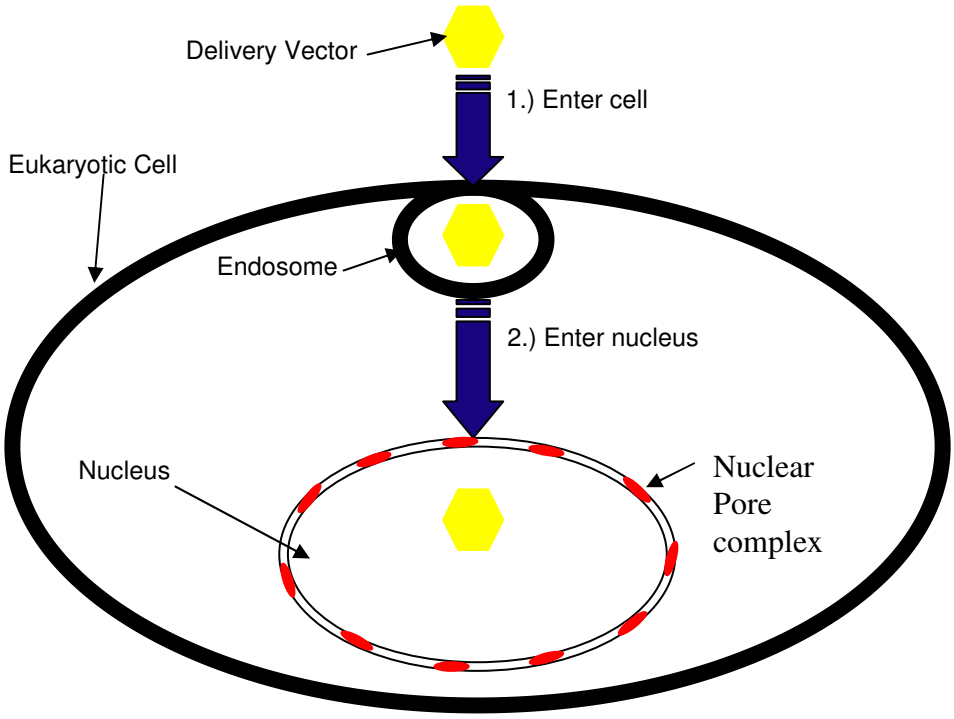

Figure 1: General scheme representing the cellular uptake and nuclear localization of a delivery vector.

The first barrier a eukaryotic cell delivery vector will encounter is the outer cell membrane. Typically, the mechanism of regulated uptake of macromolecules by a cell – endocytosis – is performed via two broad categories; phagocytosis and pinocytosis.[15] One of the pinocytotic processes of cellular uptake involves the activation of a specific receptor protein on the cell membrane surface (See Figure 2).

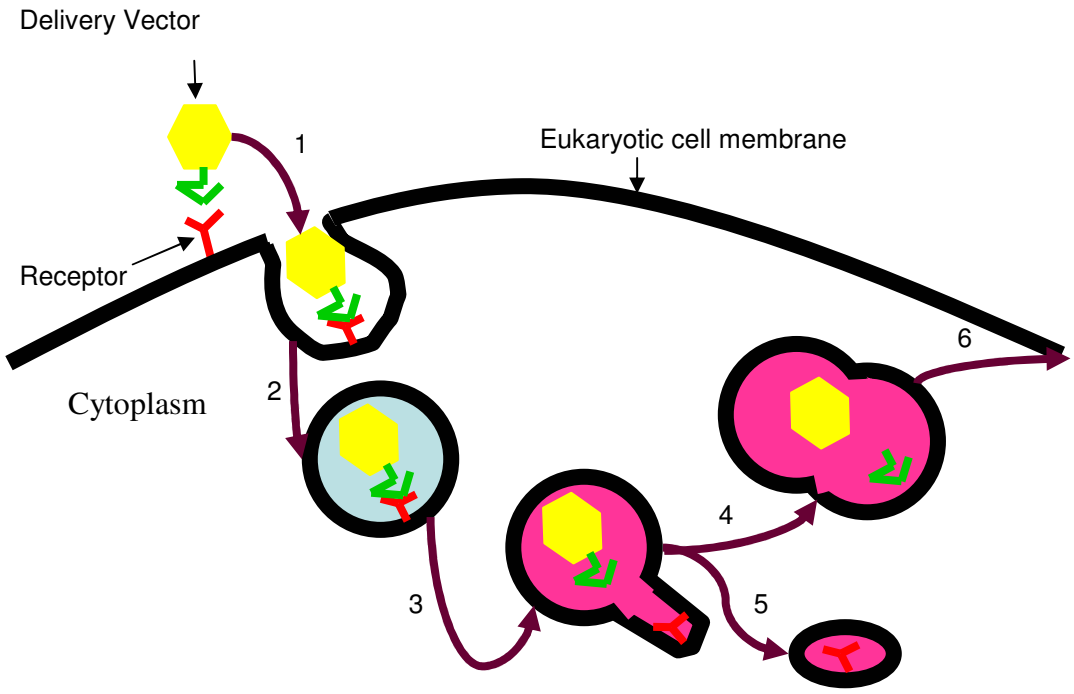

Figure 2: General representation of receptor mediated-endocytosis, with major steps (arrows) numbered.

Once activated, this receptor triggers a cascade of events leading to the invagination of the cell membrane around the receptor stimulus (via any one of a few different mechanisms), thus creating a separate compartment termed an endosome (Figure 2, Steps 1 and 2). This entire process is referred to as receptor-mediated endocytosis (RME), and is the beginning of the endosomal pathway.[14] This pathway is used by a cell for digestive purposes; that is, the endosome created undergoes several changes including an intra-compartmental drop in pH (Figure 2, Step 3) and fusion with another intracellular vesicle, a lysosome (Figure 2, Step 4)

in order to digest the endosomal contents, remove desired molecules, and allow the remainder to be discarded (Figure 2, Step 6). Cell membrane receptors are separated from the endosome prior to the endosome's fusion with a lysosome, and then recycled to the cell membrane (Figure 2, Step 5). Thus, the ultimate fate of the created endosome is re-fusion with the cell membrane to expel waste products. Clearly, if a delivery vector is designed to localize in the nucleus of a cell, then it must have some method of escaping this endosomal compartment prior to its re-fusion with the cell membrane. Many viruses contain peptide sequences which not only trigger RME, but also allow for endosomal release.

The other membranous barrier a potential delivery vector must penetrate is the nucleus itself. Nuclear membranes contain nuclear pore complexes (NPCs, Figure 3) which, when triggered, can dilate as wide as 30 nm to allow the entry (or exit) of certain materials.[10] These complexes are highly specialized; that is, only very specific molecules are allowed to pass through.

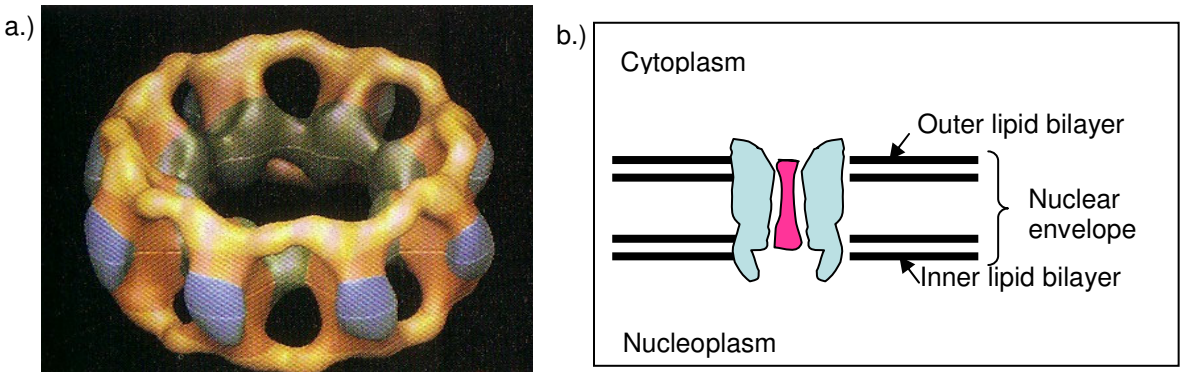

Figure 3: Representations of a nuclear pore complex. Picture a.) is a protein structural model of a nuclear pore complex [taken from Hinshaw, J.E., et al; *Cell* **1992**, *69*, 1133] and b.) is a cross-sectional schematic of a nuclear pore complex embedded in a nuclear envelope.

The first method developed using colloidal gold and biologically active peptides as a delivery vector involved a carrier protein intermediary; bovine serum albumin (BSA). Briefly, BSA was modified with many small organic linker molecules

(3-maleimido benzoic acid N-hydroxysuccinimde ester; MBS). Peptide sequences with an N-terminal cysteine residue would then be conjugated to the linker, thus cross-conjugating the peptides to the BSA. These peptide conjugates were then introduced to the gold sol in large excess (≥ 13,000 BSA : 1 colloid; Figure 4).

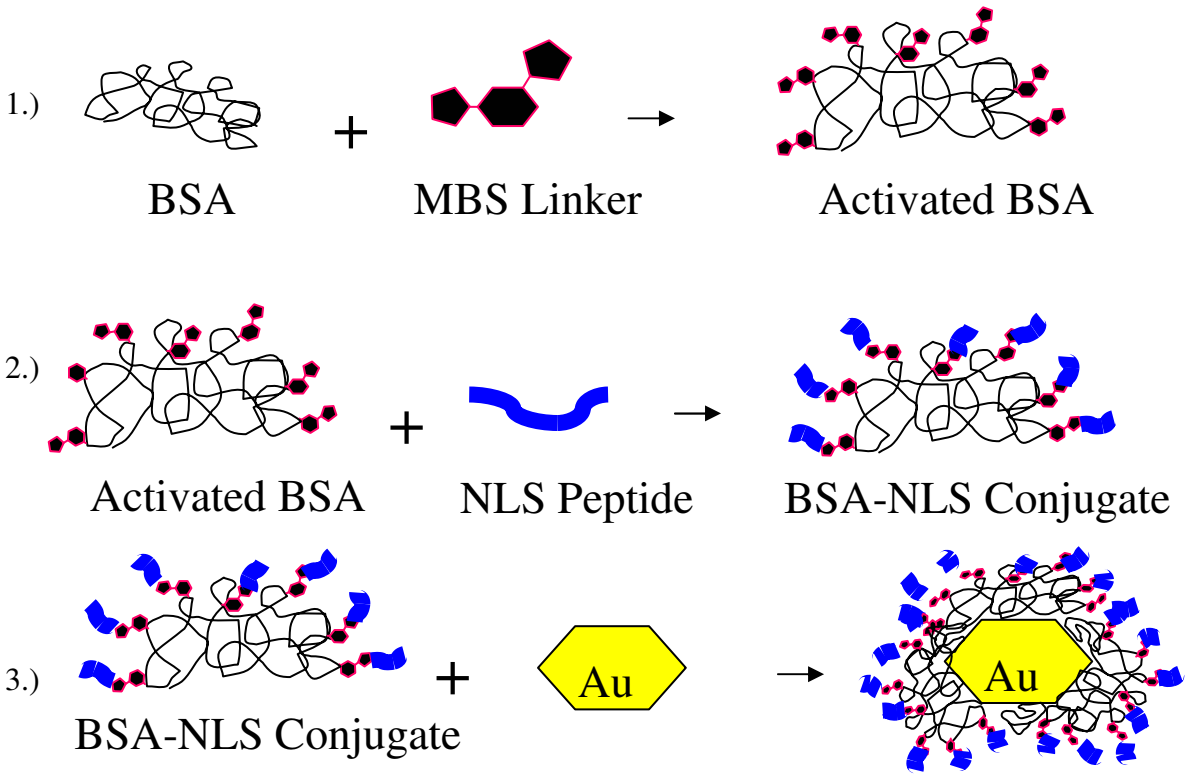

Figure 4: General scheme representing the linking of NLS peptide to BSA, then associating BSA with citrate-coated colloidal gold.

While these Au-BSA/peptide constructs have proven useful,[10,12] there are problems associated with assembling these vectors. For example, many of the Au-BSA/peptide conjugates need to be present in a large excess to maintain colloid stability in the presence of

salt. This is indicative of an equilibrium process occurring between BSA/peptide on the surface with BSA/peptide in bulk solution – removing excess BSA/peptide from solution causes BSA/peptide to disassociate with the colloidal surfaces to re-establish some equilibrium. (This phenomenon does appear to be peptide-dependant; that is, certain peptides allow more nanoparticle stability than others with/without excess BSA.) Also, if the construction of a delivery vector calls for two or more distinct peptide sequences to be used, each peptide sequence would require conjugation to independent quantities of BSA – meaning one would need to create BSA/peptide-1 separately from BSA/peptide-2, etc., and mix the resulting aliquots of BSA/peptide together in a desired ratio prior to introduction to the colloids. This is necessary because the efficiency of the addition of multiple peptide sequences to the same quantity of BSA is prohibitively low. Previous experiments[16] have tested the stability of colloidal constructs composed of peptide sequences and steric stabilizer by varying NaCl salt concentrations in solution generating Critical Coagulation Concentrations (CCC)[17] The CCC of Au-BSA colloidal constructs in solution without excess BSA was less then 3mM. This creates a real problem in using BSA as a colloidal stabilizer since the salt concentration in human blood is around 1.7M. This thesis reports the synthesis and characterization of modified polyethylene glycol as a colloidal stabilizer. Also reported are the CCC values for various mercapto-polyethylene glycol-gold-S-Au nanoparticle complexes.

Chapter 2

The idea behind the modification of polyethylene glycol was to change one end of the diol into a thiol, thus giving the needed sulfur moiety to readily attach to gold surfaces. The synthesis of thiolated polyethylene glycol is based on a modified prep previously reported from Wolfgang Tremal et al.[18] Four molecular weight polyethylene glycols were chosen for modification, there weights and corresponding ethylene glycol unit length are listed in the table below.

Polymer MW	150 Mw	400 Mw	900 Mw	1500 Mw
Peg Units	3 EG Units	9 EG Units	20 EG Units	34 EG Units

Table 1: Molecular weights and units of starting polyethylene glycol

The general reaction scheme and synthetic details are as follows. **(*p*-Tolylsulfonyl polyethylene glycol)** was synthesized by dissolving polyethylene glycol and an equal molar amount of triethylamine in acetonitrile. Next, an equal molar amount of toluene-p-sulfonyl chloride was dissolved in acetonitrile. This solution was then added dropwise over one hour. The resulting mixture was stirred for 24h at 25^{o}C. The white precipitate of triethylamine hydrochloride was filtered off and washed with acetonitrile. The solution was evaporated to dryness and the residue chromatographed from silica gel using a 10:3 ratio of chloroform and acetone. The resulting yields and starting material amounts are listed in the chart below. Proton NMR spectroscopy showed: 7.78-7.76 (d, 2H aromatic), 7.34-7.20(d, 2H aromatic), 4.15-4.12(t, 2H $O_2SOC\mathit{H}_2$), 3.68-3.56(m, $OC\mathit{H}_2$), 2.68(s, 1H, $-CH_2O\mathit{H}$), and 2.43(s, 3H, $-C\mathit{H}_3$).

PEG Mw	Amount Used g (mols)	TEA (ml)	TsCl (g)	ACN (ml)	Yield (g)	Yield (%)
150	10.0 (0.067)	9.31ml	12.78g	150ml	10.74g	52%
400	10.0 (0.025)	3.48ml	4.76g	150ml	9.32g	67%
900	10.0 (0.011)	1.53ml	2.10g	150ml	7.84g	68%
1500	10.0 (0.0067)	0.93ml	1.28g	150ml	6.43g	58%

Table 2: Amount of starting materials used and final yields in synthesis of varying length (*p*-Tolylsulfonyl polyethylene glycol

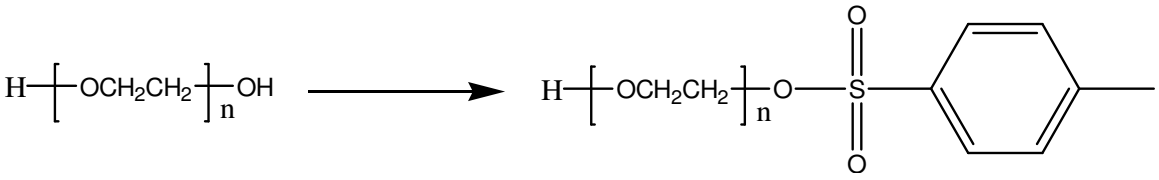

Figure 5: Structural reaction scheme of polyethylene glycol into *p*-Tolylsulfonyl polyethylene glycol)

Bromo-(polyethylene glycol) was synthesized by dissolving LiBr in reagent grade acetone. Next the Tosylated alcohol was added and the resulting mixture stirred for 5h at 80^{o}C. The mixture was then cooled to room temperature and stirred overnight. The solvent was evaporated and chloroform added to the residue. The white precipitate which formed was filtered off and the solution was washed twice with de-ionized water. The organic layer was dried over Na_2SO_4 and the solvent was evaporated. Proton NMR showed: 3.75 (t, 2H, C*H*$_2$Br), 3.68-3.56(m, OC*H*$_2$), 3.49 (t, 2H, C*H*$_2$OH), 2.68 (s, 1H, CH$_2$O*H*). The chart below shows the yields for the resulting brominated product.

PEG Mw	Ts-PEG Used g (mols)	LiBr (g)	Yield (g)	Yield %
150	10.74 g (0.035)	26.08g	4.38g	59%
400	9.32 g (0.017)	14.77g	4.21g	53%
900	7.48 g (0.0071)	6.17g	3.56g	52%
1500	6.43 g (0.0039)	3.40g	3.08g	51%

Table 3: Amount of starting materials used and final yields in synthesis of varying length Bromo-(polyethylene glycol)

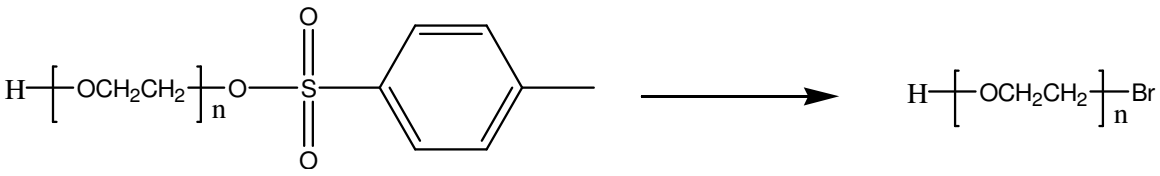

Figure 6: Structural reaction scheme *p*-Tolylsulfonyl polyethylene glycol) into Bromo-(polyethylene glycol)

Mercapto-(polyethylene glycol) was synthesized by combining the brominated polyethylene glycol with potassium thiolacetate in a 1:1.2 molar ratio in ethanol. The mixture was stirred under reflux at 80°C for 5h. The white precipitate of KBr was filtered off and the solvent evaporated. The residue was dissolved in chloroform and washed twice with water. The organic layer was dried over Na_2SO_4 and the solvent evaporated. The thiolacetate protected polyethylene glycol product was dissolved in a 1M solution of hydrochloric acid. The mixture was heated under reflux for 2h. The solvent was evaporated and the residue dissolved in chloroform. The resulting mixture was washed twice with deionized water and the organic phase dried over Na_2SO_4. Proton NMR showed: 3.74-3.58 (m, C*H*$_2$O), 3.23-3.20 (t, 2H, C*H*$_2$SH), 2.68 (s, 1H, CH$_2$O*H*), 2.16 (s, 1H, CH$_2$S*H*). The following table shows the resulting yields of the final mercapto-polyethylene glycol product.

PEG Mw	Br-PEG Used g (mols)	$KSC(O)CH_3$	Yield (g)	Yield %
150	4.38 g (0.0206)	2.83g	3.39g	98%
400	4.21 g (0.0091)	1.25g	3.70g	97%
900	3.56 g (0.0037)	0.51g	3.34g	98%
1500	3.08 g (0.0020)	0.27g	2.90g	96%

Table 4: Amount of starting materials used and final yields in synthesis of varying length Mercapto-(polyethylene glycol)

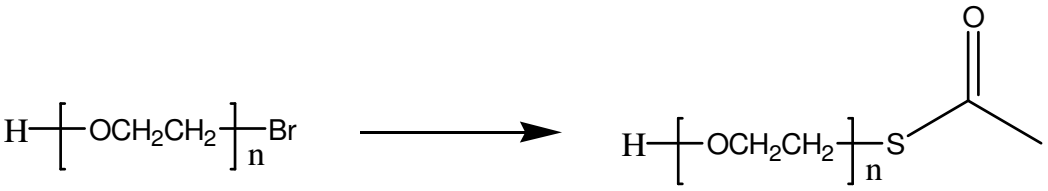

Figure 7: Structural reaction scheme of Bromo-(polyethylene glycol) into thiolacetate protected polyethylene glycol

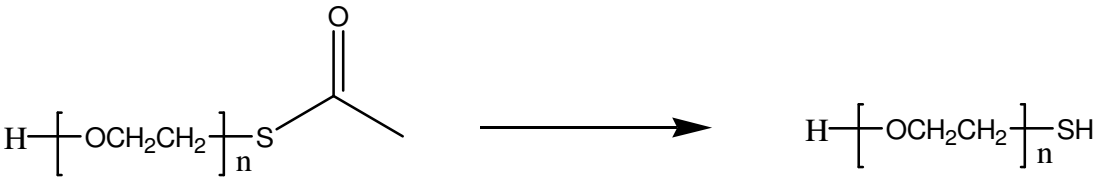

Figure 8: Structural reaction scheme of thiolacetate protected polyethylene glycol into mercapto-polyethylene glycol

Chapter 3

Now that the new mercapto-polyethylene glycols have been synthesized the next step was to attach them nanometer sized gold colloids. Attachment of polyethylene glycols to gold nanoparticles occurred via a two part mechanism. The commercially available gold nanoparticles in solution have a negatively charged citrate coating. The first step in conjugation involves removal of the citrate coating with thioctic acid.[19] The synthesis is as follows. To 1ml of commercially available citrate coated gold nanoparticles 100µl of a 0.01M solution of thioctic acid in ethanol was added. Next, 15µl of a 3M NaOH solution was added to increase the pH of the colloid solution to 11. The colloid solutions where mixed overnight on a rocking stirrer. The colloid solution was then centrifuged at 13,400rpm until the particles crashed to the bottom. The resulting supernatant was removed and the particles re-suspended in 1ml of deionized water. No color change was noted from the original red colloid citrate solution to the new thiotic acid coated particle solution. Next, 100µl of a 0.01M solution of mercapto-polyethylene glycol in ethanol was added. The pH was again adjusted to 11 with the addition of 3M NaOH. The resulting mixture was stirred overnight. The colloid solution was centrifuged at 13,400 until the particles crashed out. The supernatant was removed and the particles resuspended in Deionized water. This was done twice to maximize removal of any excess polyethylene glycol in solution. Again the color of the colloid solution remained a deep red color.

A variety of mercapto-polyethylene glycol coated gold colloids were synthesized using the method above. These complexes varied by size of nanoparticle used and length of mercapto-polyethylene glycol attached. The gold nanoparticles used were 2nm, 5nm, 10nm,

20nm, and 30nm, while the four mercapto-polyethylene glycols used where classified by molecular weights, which were 150, 400, 900, and 1500 g/mol. The Critical Coagulation Concentrations (CCC) values of the various mercapto-polyethylene glycol-gold complexes were examined. This was done by slowly adding 50µl aliquots of a 3M NaCl solution to 1ml suspensions of the mercapto-polyethylene glycol-gold complexes and calculating the final concentrations of the resulting solutions. The Critical Coagulation Concentration's were based on visual appearance of the colloid solutions after addition of the 3M NaCl. As salt is added to a gold nanoparticle solution, the colour of the colloid solution changes from a bright red to deep purple. This color change occurs as the particles begin to crash out of solution do to flocculation. As soon as any darkening of the colloidal solution was noticed the addition of the NaCl was stopped and the final concentrations of the solutions calculated. These concentrations are listed in the chart below.

Particle (nm)	Peg-SH (MW) 150 (3 mer)	400 (9 mer)	900 (20 mer)	1500 (34mer)
2	> 3M	> 3M	> 3M	> 3M
5	1.8M	> 3M	> 3M	> 3M
10	.15M	.15M	1.8M	> 3M
20	.15M	.15M	.6M	> 3M
30	.15M	.15M	.6M	> 3M

Table 5: Critical Coagulation Concentrations of various sizes of Mercapto-(polyethylene glycol) attached to various sizes of gold nanoparticles

The Critical Coagulation Concentrations showed two unique qualities about nanoparticle stabilization. First, stability of the conjugates depended on the size of nanoparticle used. The smaller the nanoparticle, the more stabile the conjugates were to increased salt concentrations. Secondly, the longer the mercapto-polyethylene glycol used (Higher Mw) showed a greater increase in stability of the gold conjugates. For 2nm Au colloids any size of mercapto-polyethylene glycol tested in the study provided the desired

stability towards the minimum salt concentration needed to stabilize the conjugates in blood. The same result was noticed for the 5nm Au colloids. When the size of the gold nanoparticle was increased to 10nm, at least a 900Mw mercapto-poly ethylene glycol was needed for adequate stability. The 20nm and 30nm Au colloids required at least a 1500Mw mercapto-poly ethylene for adequate stability.

Chapter 4

This thesis has shown the synthesis and characterization of modified polyethylene glycols and there practical use as a way of stabilizing gold nanoparticles. Critical Coagulation Concentrations for a variety of conjugates was also reported. These values provide insight into the potential use of gold nanoparticle conjugates as a viable method for cellular targeting. The conjugates synthesized of varying nanoparticle size and polymer length have shown great stability against coagulation in salt concentrations higher then that of blood. This has been the most crucial barrier against using gold nanoparticles as a viable delivery vector.

References

1. Lim, Y.; Kim, C.; Kim, K; Kim, S.W.; Park, J. *J. Am. Chem. Soc.* **2000**, *122*, 6524 – 6525.

2. Zdrahala, R.J.; Zdrahala, I.J. *J. Biomaterials Applications*, **1999**, *14(1)*, 67 – 90.

3. Boulikas, T. *Oncology Reports*. **1996**, *3(6),* 989 – 995.

4. Bilbao, G.; Gomez-Navarro, J.; Curiel, D. *Targeted Adenoviral Vectors for Cancer Gene Therapy*; Plenum Press: New York, 1998.

5. Douglas, J.T.; Curiel, D.T. *Int. J. Oncology*. **1997**, *11(2)*, 341 – 348.

6. Knoell, D.L.; Yiu, I.M. *Am. J. of Health-System Pharmacy*. **1998**, *55(9)*, 899 – 904.

7. Bubenik, J. *Int. J. Oncology*, **2001**, *18(3)*, 475 – 478.

8. Wang, J.; Mao, H.Q.; Leong, K.W. *J. Am. Chem. Soc.* **2001**, *123,* 9480 – 9481.

9. Cao, Y.; Jin, R.; Mirkin, C.A. *J. Am. Chem. Soc.***2001**, *123*, 7961 – 7962.

10. Feldherr, C.M.; Lanford, R.E.; Akin, D. *Proc. Natl. Acad. Sci. U.S.A.* **1992**, *89*, 11002-11005.

11. Schultz, S.; Smith, D.R.; Mock, J.J.; Schultz, D.A. *Proc. Natl. Acad. Sci. U.S.A.* **2000,** *97*, 996-1001.

12. Tkachenko, A.G.; Xie, H.; Coleman, D.; Glomm, W.; Ryan, J.; Anderson, M.F.; Franzen, S.; Feldheim, D.L. *J. Am. Chem. Soc.* **2003**, *125*, 4700-4701.

13. Wang, C.; Chang, K; Tang, H; Hsieh, C; Schimmel, P. *Biochemistry*, **2003**, *42*, 1646 – 1651.

14. Lodish, H.; Baltimore, D.; Berk, A.; Zipursky, S.L.; Matsudaira, P.; Darnell, J. *Molecular Cell Biology, 3rd Edition*; Scientific American Books, Inc.: New York, 1995.

15. Conner, S.D.; Schmid, S.L. *Nature*, **2003**, *422*, 37 – 44.

16. Joseph Ryan and Wilhelm Gloom

17. Shaw, D.J. *Introduction to Colloid & Surface Chemistry, 4th Edition*; Butterworth-Heinemann, Oxford, **1996**.

18. Marcus, B., Kuther, J., Nelles, G., Weber, N., Seshardi, R., and Tremel, W. *Journal of Materials Chemistry*, **1999**, 9, 1121-1125.

19. Lin., Y.S., Tsai, Y.T., Chen, C.C., Lin, C.M., Chen, C.H. *Journal of Physical Chemistry Part B,* **2004**, 108, 2134-2139.